

ChemComm

Liquid-phase synthesis of Li4GeS4 and Li10GeP2S12 electrolytes using water as the main solvent

Journal:	ChemComm	
Manuscript ID	CC-COM-09-2024-004708.R1	
Article Type:	Communication	

SCHOLARONE™ Manuscripts

ChemComm

COMMUNICATION

Liquid-phase synthesis of Li₄GeS₄ and Li₁₀GeP₂S₁₂ electrolytes using water as the main solvent

Received 00th January 20xx, Accepted 00th January 20xx

DOI: 10.1039/x0xx000000x

Hayata Tanigaki, ^a Takuya Kimura, ^a Eiji Kurioka, ^a Kota Motohashi, ^a Atsushi Sakuda, ^a Masahiro Tatsumisago ^a and Akitoshi Hayashi *^a

Liquid-phase synthesis using water as a solvent with low environmental impact was demonstrated to synthesize sulfide electrolytes. Li $_{10}\mbox{GeP}_2\mbox{S}_{12}$ was successfully synthesized and exhibited an ionic conductivity of 7.7 \times 10 $^{-3}$ S cm $^{-1}$ at 25 °C. An all-solid-state battery was fabricated using the prepared electrolyte and its reversible operation was demonstrated.

All-solid-state batteries are expected to be safe energy devices with high energy densities. Among the components used in all-solid-state batteries, solid electrolytes have been actively studied as key materials for improving their performance. Among various solid electrolyte species, $^{2-5}$ sulfide electrolytes are expected to become a desired practical material due to their high ionic conductivity and excellent formability. 6,7 In particular, the Li $_{10}$ GeP $_{2}$ S $_{12}$ (LGPS) electrolyte exhibits a room-temperature ionic conductivity of 1.2 \times 10 $^{-2}$ S cm $^{-1}$, which is comparable to that of organic electrolytes. Recently, Li $_{9.54}$ Si $_{1.74}$ P $_{1.44}$ S $_{11.7}$ Cl $_{0.3}$ and Li $_{9.54}$ Si $_{0.6}$ Ge $_{0.4}$ P $_{1.44}$ S $_{11.1}$ Br $_{0.3}$ O $_{0.6}$ with LGPS-type structures were reported to exhibit higher conductivities of 2.5 \times 10 $^{-2}$ S cm $^{-1}$ and 3.2 \times 10 $^{-2}$ S cm $^{-1}$, respectively. The compatibility of sulfide electrolytes with positive and negative electrodes has also been widely studied. $^{11-13}$

One of the drawbacks of sulfide electrolytes is their synthesis. Sulfide electrolytes are generally synthesized using solid-phase and mechanochemical methods, ^{14,15} and alternative synthesis processes that reduce energy consumption and facilitate scaling up are required. In this study, we focused on liquid-phase synthesis. The liquid-phase synthesis of LGPS has been reported by several research groups ^{16–18} and is summarised in Table 1. We focused only on the liquid-phase synthesis of LGPS from the

Table 1 List of solvents and room temperature ionic conductivities of $Li_{10}GeP_2S_{12}$ prepared by liquid-phase synthesis.

Solvents	lonic conductivity σ / S cm ⁻¹	Ref.
EtOH+THF	1.0 × 10 ⁻²	[16]
EDA+ET	1.2×10 ⁻³	[17]
ACN+THF+EtOH	1.6×10 ⁻³	[18]

starting materials and excluded preparation by the dissolution and re-precipitation of LGPS previously prepared by conventional solid-phase processes. Higashiyama et al. prepared the precursor powder by stirring P_2S_5 and Li_2S in ethanol and drying under vacuum at 80 °C. They then prepared LGPS by stirring the precursor powder, Li_2S , and GeS_2 in tetrahydrofuran (THF) for 3 days and drying under vacuum at $550\,^{\circ}\text{C}.^{16}$ A two-step liquid-phase synthesis technique was used to avoid side reactions of ethanol with P_2S_5 , which has poor moisture tolerance. Hikima et al. synthesized LGPS in 7.5 h using a mixture of acetonitrile, THF, and ethanol by adding excess sulfur. 18

In previously reported liquid-phase syntheses of LGPS, organic solvents such as alcohols, ethers, and thiols were used. This is due to the poor moisture resistance of the starting materials and sulfide solid electrolytes. The moisture resistance of sulfide electrolytes depends on the hard and soft acids and bases (HSAB) theory, 19 and the PS $_{\rm 4}^{3-}$ unit in LGPS generates H $_{\rm 2}$ S when exposed to moisture. $^{20-23}$ However, minimising the use of organic solvents is desirable because of their environmental impact and effects on the human body. Therefore, herein, we focused on using water as an environmentally friendly solvent.

In this study, we investigated the liquid-phase synthesis of LGPS using water as the solvent with the aim of preparing LGPS with less environmental impact. First, aqueous synthesis of Li_4GeS_4 , an ortho-composition solid electrolyte was performed, since

^{a.} Department of Applied Chemistry, Graduate School of Engineering, Osaka Metropolitan University, 1-1 Gakuen-cho, Naka-ku, Sakai, Osaka 599-8531, Ingan

E-mail: akitoshihayashi@omu.ac.jp

Supplementary Information available: [details of any supplementary information available should be included here]. See DOI: 10.1039/x0xx00000x

COMMUNICATION ChemComm

 ${\rm GeS_4}^{4-}$ units are contained in LGPS. Next, LGPS was synthesized in the liquid phase by combining reacting aqueous solution of ${\rm Li_4GeS_4}$ with THF suspension of ${\rm Li_3PS_4}$. The structures of the prepared samples were characterized using X-ray diffraction (XRD) and Raman spectroscopy, and the ionic conductivities of the samples were measured using alternating current (AC) impedance. An all-solid-state cell was constructed using the prepared LGPS electrolyte, and its properties were evaluated. Detailed synthesis and characterization procedures are described in Supporting Information.

The liquid-phase synthesis of Li₄GeS₄ was carried out using water as the solvent and GeS₂ or Ge as the starting Ge source. The starting materials of Li₂S, S and GeS₂ or Ge, were weighed to obtain stoichiometric compositions. Deionized water was added to the mixture of the starting materials under atmospheric conditions and stirred at 80 °C for 6 h. Fig. 1a and b show photographs of the precursor solutions prepared using Ge or GeS₂, respectively. A uniform solution was not formed when Ge was used as a starting material, and precipitates remained. In contrast, a clear aqueous solution was obtained using GeS2. Fig. 1c shows the XRD patterns of the prepared samples after drying under vacuum at 200 °C for 3 h. The sample prepared using Ge exhibited an XRD pattern attributable to Ge, indicating that unreacted Ge remained. The XRD pattern of the sample prepared using GeS₂ was attributed to Li₄GeS₄. Therefore, Li₄GeS₄ was successfully liquid-phase-synthesized using GeS₂ as the starting material. These results indicate that in the aqueous synthesis, Li₂S is first dissolved in water to form a basic aqueous solution, and the other starting materials must

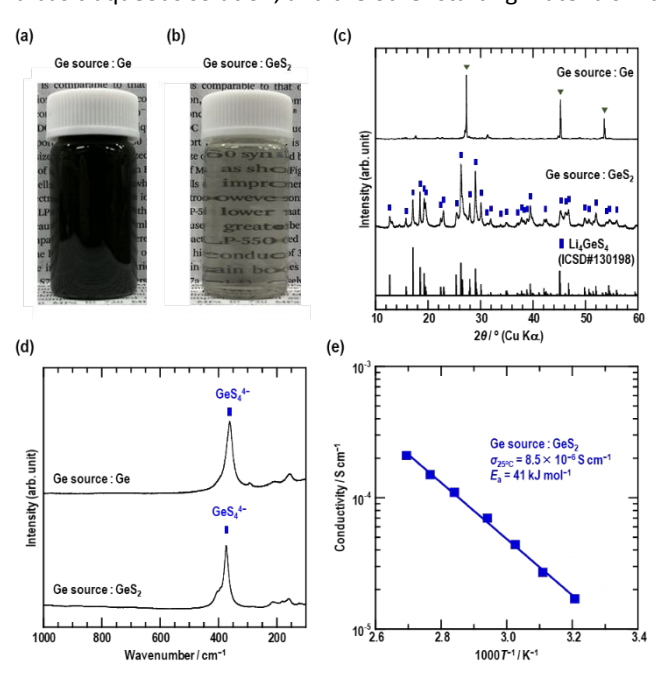


Fig. 1 (a) Photographs of the precursor prepared using Li₂S, sulfur, and two different Ge sources: (a) Ge metal and (b) GeS₂. (c) XRD patterns, (d) Raman spectra and (e) temperature dependence of the ionic conductivity of Li₄GeS₄ prepared by liquid-phase synthesis using water as the solvent.

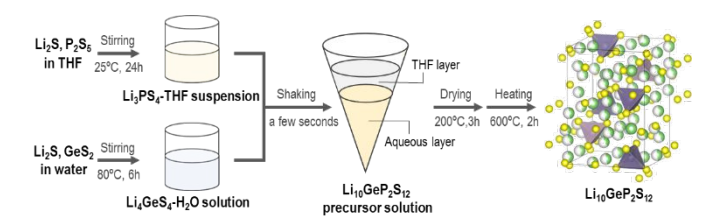


Fig. 2 Synthetic scheme for synthesizing $\rm Li_{10}GeP_2S_{12}$ electrolytes from $\rm Li_4GeS_4$ - $\rm H_2O$ solution and $\rm Li_3PS_4$ -THF suspension.

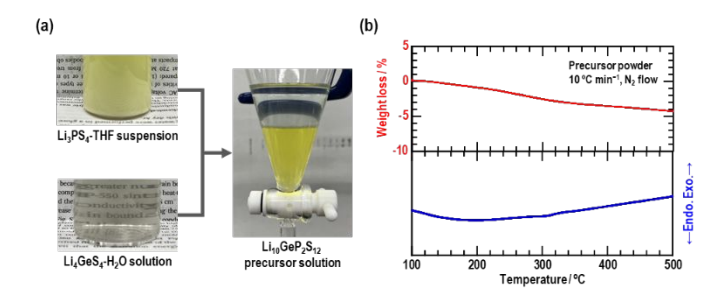


Fig. 3 (a) Photographs of Li_4GeS_4 - H_2O solution and Li_3PS_4 -THF suspension after 6 or 24 h stirring, and of the $Li_{10}GeP_2S_{12}$ precursor solution after being shaken in a separation funnel. (b) TG-DTA curves of the $Li_{10}GeP_2S_{12}$ precursor powder after heat treatment under vacuum at 200 $^{\circ}C$.

be soluble in the basic solution.

The moisture tolerance of sulfide electrolytes depends on the HSAB theory, and sulfide electrolytes with a soft acid such as Li_4SnS_4 or Na_3SbS_4 as the central metal show high moisture tolerance. ^{24–28} In this study, Li_4GeS_4 with Ge as the central metal was found to exhibit high moisture tolerance.

Fig. 1d shows the Raman spectra of the obtained samples. The band attributed to GeS_4^{4-} was observed in both Ge and GeS_2 , indicating that a small amount of Ge reacts to form GeS_4^{4-} when Ge is used as the starting material. Fig. 1e shows the temperature dependence of the ionic conductivity of Li_4GeS_4 . The room temperature conductivity of Li_4GeS_4 was 8.5×10^{-6} S cm⁻¹ and the activation energy for conduction was 41 kJ mol⁻¹.

The synthesis of LGPS was performed by combining the aqueous solution synthesis of Li₄GeS₄ described above with the previously reported liquid-phase synthesis of Li₃PS₄.²⁹ The synthesis scheme of the LGPS electrolyte is shown in Fig. 2. The Li₃PS₄—THF suspension was prepared by adding stoichiometric ratios of Li₂S and P₂S₅ to THF and stirring at room temperature for 1 day. The resulting Li₃PS₄—THF suspension and the above Li₄GeS₄ aqueous solution were quickly mixed in a few seconds using a separating funnel. The separated aqueous layer was vacuum dried at 200°C, followed by heat treatment at 600°C for 2 h. Fig. 3a shows photographs of the precursors obtained in the synthesis process. A LGPS precursor solution was formed in the aqueous layer by mixing the Li₃PS₄—THF precursor suspension and an aqueous precursor solution of Li₄GeS₄ in a separating funnel. A clear, colourless THF layer formed as the oil layer.

Journal Name COMMUNICATION

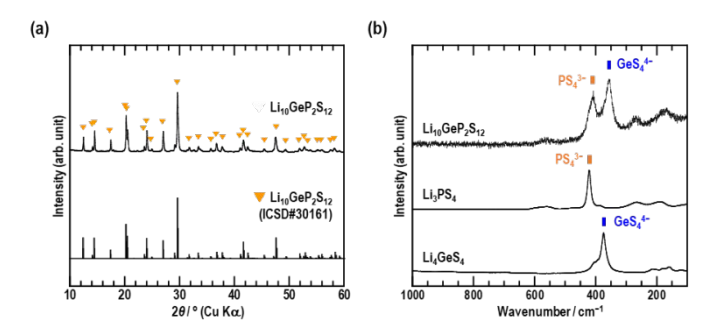


Fig. 4 (a) XRD pattern of Li_{10} GeP₂S₁₂ prepared by liquid-phase synthesis using water as the solvent. (b) Raman spectra of Li_{10} GeP₂S₁₂, Li_3 PS₄ and Li_4 GeS₄ powders. The samples of Li_{10} GeP₂S₁₂ and Li_4 GeS₄ were prepared by liquid-phase synthesis.

Although water and THF are completely miscible, Li_2S and GeS_2 were dissolved in water to form a Li_4GeS_4 solution, which increased the polarity of the aqueous layer, which resulted in the separation of the water and THF layers.

Fig. S1 shows the Raman spectrum of the THF layer after mixing. No bands attributed to the PS_4^{3-} unit are present, indicating that the Li_3PS_4 component in the THF suspension was almost completely extracted into the aqueous layer. Although water and THF were used as solvents in this study, THF was recovered during the synthesis process and few organic solvents were released into the environment. These suggest that THF used as the solvent can be recovered and reused.

The obtained LGPS precursor solution was dried under vacuum at 200 °C, in the same manner as that used for the synthesis of Li_4GeS_4 , to obtain the precursor powder. Its XRD pattern is mainly attributed to Li_3PS_4 as shown in Fig. S2. Fig. 3b shows the TG-DTA curves of the obtained precursor powder after drying at 200 °C. The sample of LGPS was prepared by heat treatment at 600 °C because no peak originating from the precipitation of LGPS was observed following the heat treatment at 500 °C.

The particle sizes and shapes of the electrolytes are important for mixing the active materials in the fabrication of all-solid-state cells. The SEM image of LGPS is shown in Fig. S3. The sample particles after drying under vacuum were angular with a particle of less than 2 μ m. Furthermore, the crystal growth of electrolytes was achieved by heat treatment at 600 °C, and the size of the resulting rounded particle was 1–5 μ m.

The XRD pattern of the as-prepared sample is shown in Fig. 4a, which was attributed to LGPS and no impurities associated with the oxidation of P was observed. The PS_4^{3-} unit, which is not moisture resistant, generates H_2S when reacted with water. In this study, PS_4^{3-} units remained by quickly mixing in a few seconds of the Li_3PS_4 —THF suspension and the Li_4GeS_4 aqueous solution. Furthermore, the Li_4GeS_4 aqueous solution is basic, which is also important for inhibiting the formation of H_2S and the hydrolysis of PS_4^{3-} . Fig. 4b shows the Raman spectrum of the prepared LGPS, showing bands attributed to GeS_4^{4-} at 365 cm⁻¹ and PS_4^{3-} at 420 cm⁻¹. 30,31 The band attributed to the PO_4^{3-} units

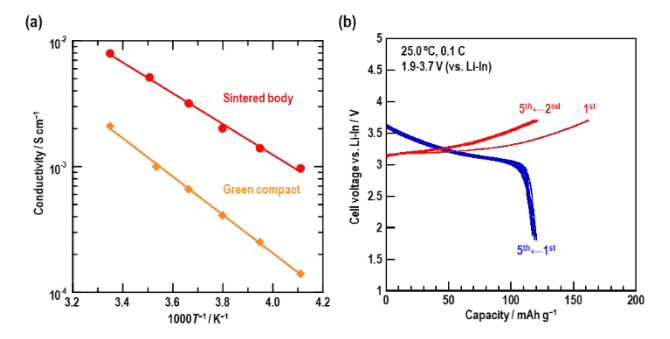


Fig. 5 (a) Temperature dependence of conductivities of $Li_{10}GeP_2S_{12}$ prepared by liquid-phase synthesis using water as the solvent. (b) Charge–discharge curves of the Li-In/Li₁₀GeP₂S₁₂/NMC cell with the conventional mixed electrode prepared by the hand-mixing of NMC and $Li_{10}GeP_2S_{12}$ particles using a mortar.

at approximately 940 cm $^{-1}$ 32 was not observed, indicating that the PS $_4$ 3- unit was hardly hydrolyzed. The liquid-phase synthesis of LGPS was achieved using water as the solvent.

AC impedance measurements were performed to determine the ionic conductivities of the prepared LGPS samples. The temperature dependence of ionic conductivity is shown in Fig. 5a. Green compacts formed at 360 MPa exhibited a relative density of 71%, ionic conductivity of 2.0 × 10⁻³ S cm⁻¹ at 25 °C, and activation energy of 29 kJ mol⁻¹. Sintering the green compacts at 600 °C in a dry Ar atmosphere increased the relative density to 91% and the ionic conductivity to 7.7×10^{-3} S cm⁻¹, while the activation energy decreased to 26 kJ mol⁻¹. The LGPS electrolytes prepared in this study exhibited high conductivities that are comparable to those prepared by conventional solid-state reactions. The temperature dependence of the ionic conductivities of the samples prepared in this experiment are shown in Fig. S4, and the roomtemperature ionic conductivities, activation energies, and relative densities are summarised in Table S1. The LPGS prepared here has slightly lower conductivity than the LGPS prepared using THF and ethanol as solvents reported by Higashiyama et al. 16 They prepared LGPS in a two-step synthetic process in which the PS₄³⁻ unit was not in direct contact with ethanol. By avoiding the side reaction of the PS₄³⁻ unit with ethanol, the higher ionic conductivity was presumably achieved in the previous report. Since differences in the surface and morphology of prepared LGPS affect their conductivity, detailed structural analyses are important to understand ionic conduction in electrolytes prepared by liquid phase processes.

All-solid-state cells were fabricated using the prepared LGPS electrolyte as a separator layer and as an electrolyte of NMC composite positive electrode. The charge—discharge curves of the all-solid-state cell are shown in Fig. 5b. The cell was operated as a secondary battery, demonstrating that LGPS prepared via liquid-phase synthesis can be used as a solid electrolyte in all-solid-state batteries. At the initial cycle, an irreversible capacity was observed. The cause of the low Coulombic efficiency is probably on the NMC positive electrode

COMMUNICATION ChemComm

side, since the all-solid-state cell with TiS_2 positive electrode showed better reversibility at the first cycle, as shown in Fig. S5. Partial side-reaction of LGPS at the interface with NMC may be the cause of the low Coulomb efficiency. After the 2^{nd} cycle, the cells with both NMC and TiS_2 as positive electrodes retained reversible capacities for 5 cycles.

In conclusion, we report the liquid-phase syntheses of Li_4GeS_4 and LGPS using water as the solvent with the aim of establishing a simple and environmentally friendly synthesis method. Li_4GeS_4 was synthesized from Li_2S and GeS_2 using water as the solvent. LGPS was synthesized by combining the Li_4GeS_4 aqueous solution with a Li_3PS_4 —THF suspension. The XRD pattern of the prepared sample was attributed to $Li_{10}GeP_2S_{12}$, indicating that the liquid-phase synthesis of LGPS was achieved using water as the solvent. The prepared sample exhibited an ionic conductivity of 7.7×10^{-3} S cm $^{-1}$ at room temperature, and the all-solid-state cell fabricated using the prepared LGPS as the solid electrolyte and positive electrode could be operated reversibly. In this study, we developed a new method for the liquid-phase synthesis of LGPS with a low environmental impact and demonstrated new possibilities for liquid-phase synthesis.

Conflicts of interest

There are no conflicts to declare.

Data availability

The data are available from the corresponding author on reasonable request.

Acknowledgements

This work was financially supported by the Japan Science and Technology Agency ALCA-SPRING and GteX projects (grant numbers JPMJAL1301 and JPMJGX23S5), and the Japan Society for the Promotion of Science KAKENHI (grant number JP19H05816).

References

- 1 A. Manthiram, X. Yu and S. Wang, *Nat. Rev. Mater.*, 2017, **2**, 16103
- D. Park, H. Park, Y. Lee, S.-O. Kim, H.-G. Jung, K. Y. Chung, J. H. Shim and S. Yu, ACS Appl. Mater. Interfaces, 2020, 12, 34806–34814.
- 3 H. Kwak, S. Wang, J. Park, Y. Liu, K. T. Kim, Y. Choi, Y. Mo and Y. S. Jung, ACS Energy Lett., 2022, 7, 1776–1805.
- 4 E. Quartarone and P. Mustarelli, *Chem. Soc. Rev.*, 2011, **40**, 2525–2540.
- 5 F. Zheng, M. Kotobuki, S. Song, M. O. Lai and L. Lu, J. Power Sources, 2018, 389, 198–213.
- 6 A. Sakuda, A. Hayashi and M. Tatsumisago, Sci. Rep., 2013, 3, 2261.
- A. Kato, M. Nose, M. Yamamoto, A. Sakuda, A. Hayashi and M. Tatsumisago, J. Ceram. Soc. Japan, 2018, 126, 719–727.

- 8 N. Kamaya, K. Homma, Y. Yamakawa, M. Hirayama, R. Kanno, M. Yonemura, T. Kamiyama, Y. Kato, S. Hama, K. Kawamoto and A. Mitsui, *Nat. Mater.*, 2011, **10**, 682–686.
- 9 Y. Kato, S. Hori, T. Saito, K. Suzuki, M. Hirayama, A. Mitsui, M. Yonemura, H. Iba and R. Kanno, *Nat. Energy*, 2016, **1**, 16030.
- 10 Y. Li, S. Song, H. Kim, K. Nomoto, H. Kim, X. Sun, S. Hori, K. Suzuki, N. Matsui, M. Hirayama, T. Mizoguchi, T. Saito, T. Kamiyama and R. Kanno, *Science*, 2023, **381**, 50–53.
- 11 J. Wu, L. Shen, Z. Zhang, G. Liu, Z. Wang, D. Zhou, H. Wan, X. Xu and X. Yao, *Electrochem. Energy Rev.*, 2021, **4**, 101-135.
- 12 S. Jeong, Y. Li, W.H. Sim, J. Mun, J.K. Kim and H.M. Jeong, *EcoMat.*, 2023, 5, e12338.
- 13 J. Zheng, X. Zhu, L. Wang, J. Lu and T. Wu, *Mater. Chem. Front.*, 2023, **7**, 4810-832.
- 14 A. Hayashi, S. Hama, H. Morimoto, M. Tatsumisago and T. Minami, *J. Am. Ceram. Soc.*, 2001, **84**, 477–479.
- 15 K. Suzuki, D. Kato, K. Hara, T. Yano, M. Hirayama, M. Hara and R. Kanno, *Electrochim. Acta*, 2017, **258**, 110–115.
- 16 Y. Higashiyama, T. Nakagawa and N. Machida, *J. Jpn Soc. Powder Powder Metallurgy.*, 2022, **69**, 117–120.
- 17 J. E. Lee, K. H. Park, J. C. Kim, T. U. Wi, A. R. Ha, Y. B. Song, D. Y. Oh, J. Woo, S. H. Kweon, S. J. Yeom, W. Cho, K. Kim, H. W. Lee, S. K. Kwak and Y. S. Jung, *Adv. Mater.*, 2022, **34**, e2200083.
- 18 K. Hikima, K. Ogawa, H. Gamo and A. Matsuda, *Chem. Commun.*, 2023, **59**, 6564–6567.
- 19 G. Sahu, Z. Lin, J. Li, Z. Liu, N. Dudney and C. Liang, *Energy Environ. Sci.*, 2014, 7, 1053–1058.
- 20 H. Muramatsu, A. Hayashi, T. Ohtomo, S. Hama and M. Tatsumisago, *Solid State Ion*, 2011, **182**, 116–119.
- 21 W. D. Jung, M. Jeon, S. S. Shin, J.-S. Kim, H.-G. Jung, B.-K. Kim, J.-H. Lee, Y.-C. Chung and H. Kim, ACS Omega, 2020, 5, 26015–26022.
- 22 A. Hayashi, H. Muramatsu, T. Ohtomo, S. Hama and M. Tatsumisago, *J. Mater. Chem. A*, 2013, **1**, 6320.
- 23 T. Nakano, T. Kimura, A. Sakuda, M. Tatsumisago and A. Hayashi, *J. Phys. Chem. C*, 2022, **126**, 7383–7389.
- 24 H. Wang, Y. Chen, Z. D. Hood, G. Sahu, A. S. Pandian, J. K. Keum, K. An and C. Liang, *Angew. Chem. Int Ed Engl*, 2016, 55, 8551–8555.
- 25 T. Kaib, P. Bron, S. Haddadpour, L. Mayrhofer, L. Pastewka, T. T. Järvi, M. Moseler, B. Roling and S. Dehnen, *Chem. Mater.*, 2013, 25, 2961–2969.
- 26 A. Banerjee, K. H. Park, J. W. Heo, Y. J. Nam, C. K. Moon, S. M. Oh, S. T. Hong and Y. S. Jung, *Angew. Chem. Int Ed Engl*, 2016, 55, 9634–9638.
- 27 K. Kanazawa, S. Yubuchi, C. Hotehama, M. Otoyama, S. Shimono, H. Ishibashi, Y. Kubota, A. Sakuda, A. Hayashi and M. Tatsumisago, *Inorg. Chem.*, 2018, 57, 9925–9930.
- 28 T. Kimura, T. Nakano, A. Sakuda, M. Tatsumisago and A. Hayashi, *J. Phys. Chem. C*, 2023, **127**, 1303–1309.
- 29 Z. Liu, W. Fu, E. A. Payzant, X. Yu, Z. Wu, N. J. Dudney, J. Kiggans, K. Hong, A. J. Rondinone and C. Liang, *J. Am. Chem. Soc.*, 2013, **135**, 975–978.
- M. Tachez, J. Malugani, R. Mercier and G. Robert, *Solid State Ion*, 1984, 14, 181–185.
- 31 W. Yao, K. Berg and S. Martin, *Journal of Non-Crystalline Solids*, 2008, **354**, 2045–2053.
- 32 L. Popović, B. Manoun, D. de Waal, M. K. Nieuwoudt and J. D. Comins, *J. Raman Spectroscopy*, 2003, **34**, 77–83.

Page 5 of 5 ChemComm

Data availability statements

The data are available from the corresponding author on reasonable request.